REPORT DOCUMENTATION PAGE

Form Approved
OMB No. 0704-0188

1. REPORT DATE *(DD-MM-YYYY)*	2. REPORT TYPE	3. DATES COVERED *(From - To)*
03/24/2011	Final Report	3/15/05 to 9/30/10

4. TITLE AND SUBTITLE
Energy Budget of Nonlinear Internal Waves near DongSha

5a. CONTRACT NUMBER

5b. GRANT NUMBER
N00014-05-1-0284

5c. PROGRAM ELEMENT NUMBER

6. AUTHOR(S)
Ren-Chieh Lien; Eric D'Asaro; Frank Henyey; Ming-Huei Chang; Dajun Tang; Jie Yang.

5d. PROJECT NUMBER

5e. TASK NUMBER

5f. WORK UNIT NUMBER

7. PERFORMING ORGANIZATION NAME(S) AND ADDRESS(ES)
Applied Physics Laboratory
University of Washington
NE 40th Street
Seattle, WA 98105

8. PERFORMING ORGANIZATION REPORT NUMBER

9. SPONSORING/MONITORING AGENCY NAME(S) AND ADDRESS(ES)
Theresa Paluszkiewicz, ONR
Office of Naval Research
875 North Randolph Street
Arlington, VA 22203-1995

10. SPONSOR/MONITOR'S ACRONYM(S)
ONR

11. SPONSOR/MONITOR'S REPORT NUMBER(S)

12. DISTRIBUTION/AVAILABILITY STATEMENT
Approved for public release; distribution is unlimited

13. SUPPLEMENTARY NOTES

14. ABSTRACT
Our long-term scientific goal is to understand the mechanisms by which mixing occurs in the ocean and thereby help develop improved parameterizations of mixing for ocean models. Mixing within the stratified ocean is our particular focus as the complex interplay of internal waves from a variety of sources and turbulence makes this a current locus of uncertainty. In this study, our broad focus is on the energy sources of nonlinear internal waves (NLIWs) in a complex environment of strong internal tides and abrupt topography (continental shelf and slope). We expect a rapid evolution of internal tides and NLIWs, and aim to understand their dynamics, energy cascade, and role in mixing

15. SUBJECT TERMS

16. SECURITY CLASSIFICATION OF:			17. LIMITATION OF ABSTRACT	18. NUMBER OF PAGES	19a. NAME OF RESPONSIBLE PERSON
a. REPORT	b. ABSTRACT	c. THIS PAGE			Ren-Chieh Lien
U	U	U	UU	11	19b. TELEPHONE NUMBER *(Include area code)* (206) 685-1079

Energy Budget of Nonlinear Internal Waves near Dongsha

Ren-Chieh Lien
Applied Physics Laboratory
University of Washington
1013 NE 40th Street
Seattle, Washington 98105
phone: (206) 685-1079 fax: (206) 543-6785 email: lien@apl.washington.edu

Award Number: N00014-05-1-0284

LONG-TERM GOALS

Our long-term scientific goal is to understand the mechanisms by which mixing occurs in the ocean and thereby help develop improved parameterizations of mixing for ocean models. Mixing within the stratified ocean is our particular focus as the complex interplay of internal waves from a variety of sources and turbulence makes this a current locus of uncertainty. In this study, our broad focus is on the energy sources of nonlinear internal waves (NLIWs) in a complex environment of strong internal tides and abrupt topography (continental shelf and slope). We expect a rapid evolution of internal tides and NLIWs, and aim to understand their dynamics, energy cascade, and role in mixing.

OBJECTIVES

The primary objectives of this project are 1) to identify the generation site and understand the generation mechanism of NLIWs, 2) to understand the evolution of NLIWs as they interact with abrupt topography, 3) to quantify the energy budget and energy cascade from internal tides to NLIWs, and 4) to quantify the seasonal variation of the energy of NLIWs near Dongsha Plateau in the northern South China Sea (SCS). Our particular interest is to understand the energy cascade from barotropic tides, internal tides, and NLIWs to turbulence mixing in the northern SCS, and to understand the evolution of NLIWs interacting with the shoaling continental slope.

APPROACH

Our approach is to make direct observations of NLIWs near Dongsha Island where NLIWs are often captured in satellite images. Primary platforms include an ADV Lagrangian Float, an array of bottom-mounted ADCP moorings, and shipboard EK500, marine radar, ADCP, and CTD. Our main goals are to quantify the energy budget and evolution of NLIWs across the rapidly shoaling continental slope and the gentle plateau near Dongsha Island and to quantify seasonal variations of NLIW characteristics.

WORK COMPLETED

We have completed three components of this observational experiment: 1) pilot observations in 2005, 2) extended observations in 2006–2007, and 3) intensive observations in 2007.

Pilot Observations (April 2005)

In April 2005 we conducted a two-week observational experiment near Dongsha (Fig. 1). Large-amplitude NLIWs, greater than 150 m, and strong turbulence mixing were observed by the Lagrangian float and shipboard sensors including ADCP, CTD, EK500, and X-band marine radar. Combined remote sensing and in-situ measurements provided detailed properties of large-amplitude NLIWs.

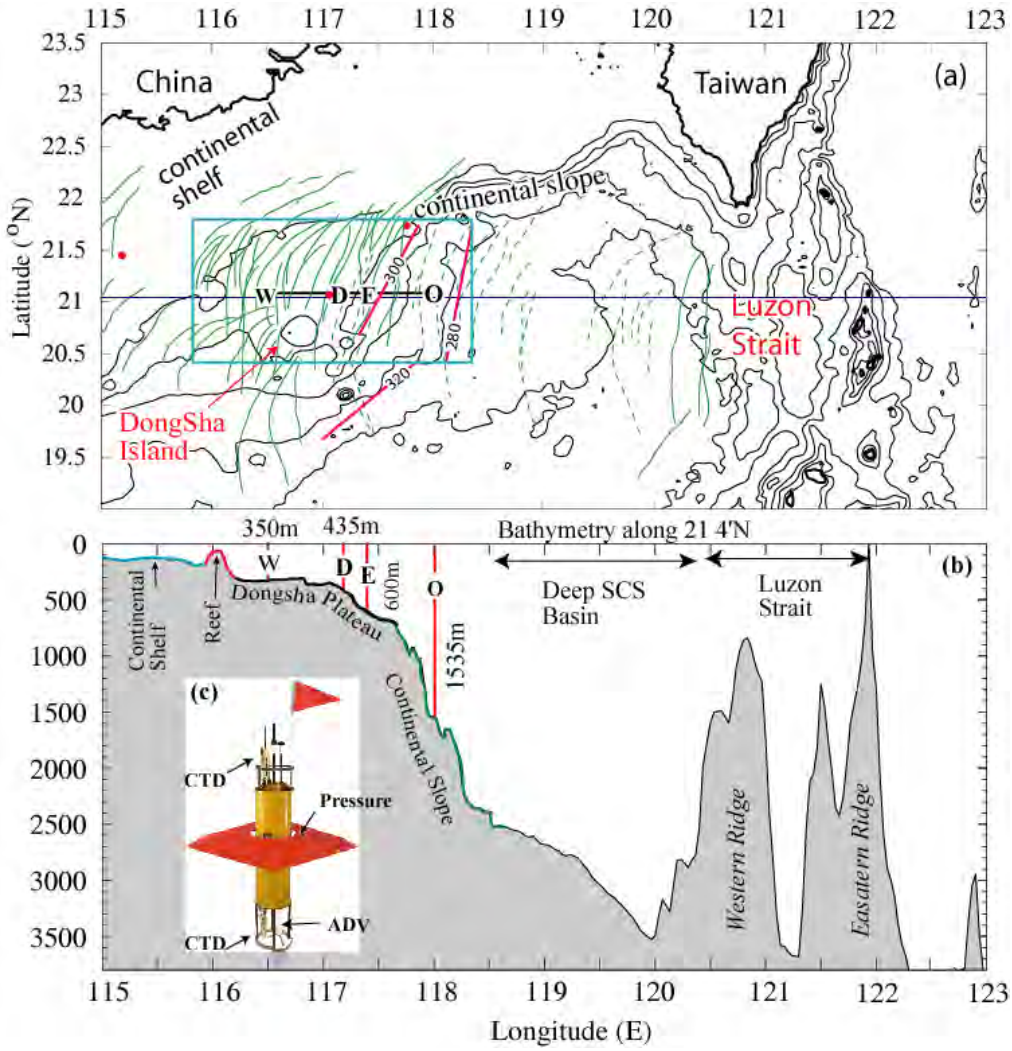

Figure 1: (a) Map of the northern South China Sea, and (b) bottom bathymetry along 21°4'N. In (a) green curves represent surface signatures of NLIWs identified in satellite images (Zhao et al. 2004), dashed for single-depression waves and solid for multiple wave packets. The blue box delineates the area where multiple wave packets are mostly found. Four primary stations in our April–May 2005 cruise are labeled as O, E, D and W. Shipboard and float measurements were taken along O-E-D-W. Three magenta curves illustrate isobaric orientations on the continental slope. In panel (b) two submarine ridges in the Luzon Strait are labeled. They are responsible for generating strong internal tides. Depths at four primary stations are also labeled. The inset (c) shows the Lagrangian float and sensors equipped on the float.

Extended ADCP Observations (June 2006–May 2007)

An array of three ADCP moorings was deployed along the prevailing path of NLIWs near Dongsha in June 2006 (Fig. 2). Three ADCPs were serviced once and recovered in May 2007. Two of three moorings took velocity measurements for about 11 months. These long-term observations of NLIWs allow us to 1) quantify the seasonal variation of NLIW energy, 2) map the geographical distribution, 3) better understand the dynamics of NLIW evolution over the shoaling topography, and (4) assess the model prediction skill for NLIWs.

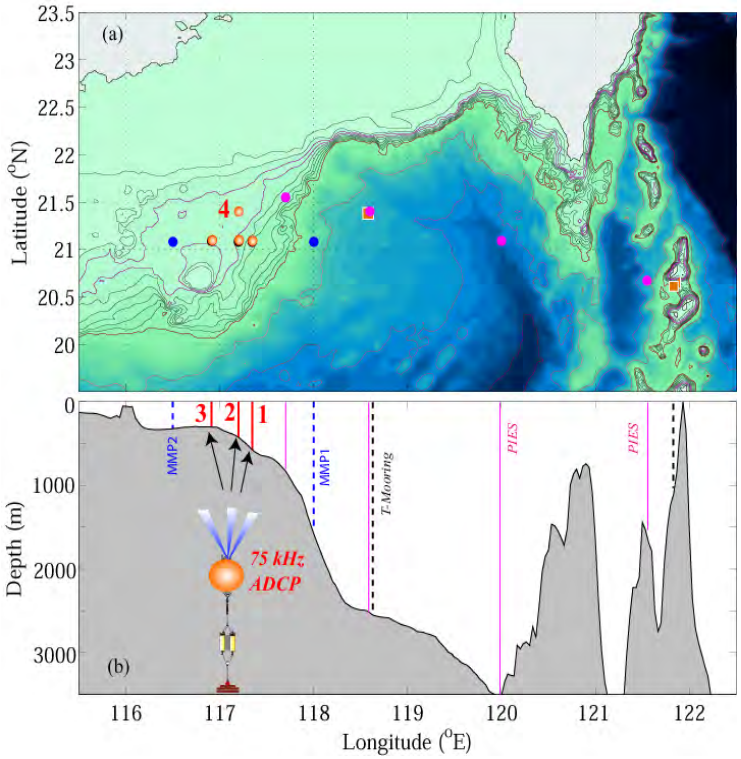

Figure 2: (a) Map of South China Sea and (b) bathymetry along 21°N. Four yellow bullets and red lines mark the locations of moored ADCPs. The configuration of the bottom-mounted 75-kHz ADCP is shown in (b). Two blue dots (vertical blue dashed lines), magenta dots (vertical magenta lines), and brown squares (vertical black dashed lines) mark the positions of McLane moored profilers (Alford), PIES (Farmer), and temperature moorings (Tang and Ramp), respectively. Labels 1–4 represent the moored ADCPs.

Intensive Observations (April–May 2007)

We participated in the multi-ship intensive observation experiment near Dongsha in April–May 2007. Another bottom-mounted ADCP mooring was deployed on Dongsha Plateau to help acousticians understand the effects of NLIWs on acoustic propagation. Our main goals were to understand the interaction of internal waves, including internal tides and NLIWs, with the rapidly shoaling continental slope, and to quantify the energy budget of internal waves near Dongsha. Our primary instruments included Scripps Institution's fast CTD profiler, and shipboard ADCP, CTD, EK500, and marine radar. During the cruise two McLane moored profilers were deployed, one on the continental slope and the other on Dongsha Plateau (Fig. 2).

RESULTS

Supported by this project, five papers have been published (Lien et al. 2005, Chang et al. 2006, Moore and Lien 2007, Chang et al. 2008, Chang et al. 2011), one paper (Lien et al. 2011) is under review, and two more papers are in preparation. There are many co-authored papers. Significant results presented in them are:

Bio-Physical Coupling: Pilot Whales Follow NLIWs in the SCS (Moore and Lien 2007)

Schools of pilot whales were observed behind the large-amplitude NLIWs. Moore and Lien (2007) proposed that prey availability for pilot whales in the SCS is influenced by the aggregative properties of NLIWs (Fig. 3). This is the first report of cetaceans associated with internal waves. We expect that the ecosystem in the SCS is strongly modulated by NLIWs.

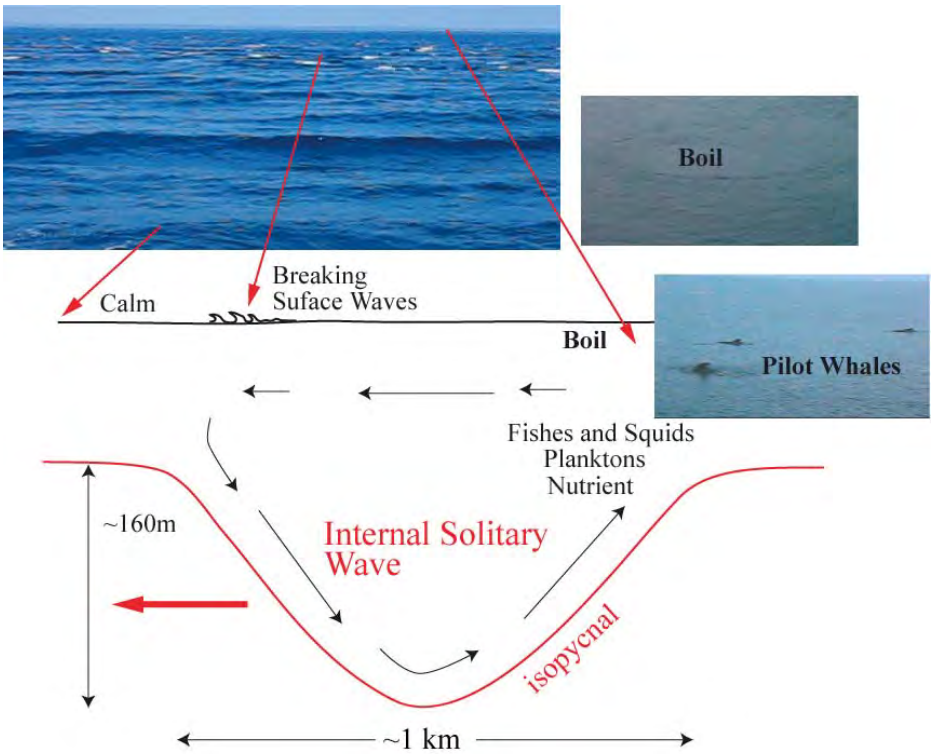

Figure 3: Snapshorts of varying sea-surface conditions associated with internal waves coupled to a schematic diagram showing the spatial scale and currents associated with an observed NLIW. Strong downwelling in the front portion of the internal wave creates breaking surface waves; upwelling in the rear portion of the wave, where the pilot whales were seen, creates surface boils and may entrain fishes, squids, plankton, and nutrients.

Energy Budget on Dongsha Plateau (Lien et al. 2005, Chang et al. 2006)

Historical mooring data are used to compute the energy flux of NLIWs across Dongsha Plateau (Chang et al. 2006). Strong divergence of energy and energy flux of NLIWs are observed along and across waves' prevailing westward propagation path (Fig. 4). The NLIW energy flux is 8.5 kW m^{-1} on the plateau, 0.25 kW m^{-1} on the continental shelf 220 km westward along the propagation path, and 1 kW m^{-2} on the continental slope 120 km northward across the propagation path. Along the wave path on

the plateau, the average energy flux divergence of NLIW is ~0.04 W m^{-2}, which corresponds to a dissipation rate of O(10^{-7} – 10^{-6}) W kg^{-1} for NLIWs. Combining these observations and model results creates a scenario of NLIW energy flux in the SCS. NLIWs are generated east of the plateau, propagate predominantly westward across the plateau along a beam of ~100 km width that is centered at ~21°N, and dissipate nearly all their energy before reaching the continental shelf.

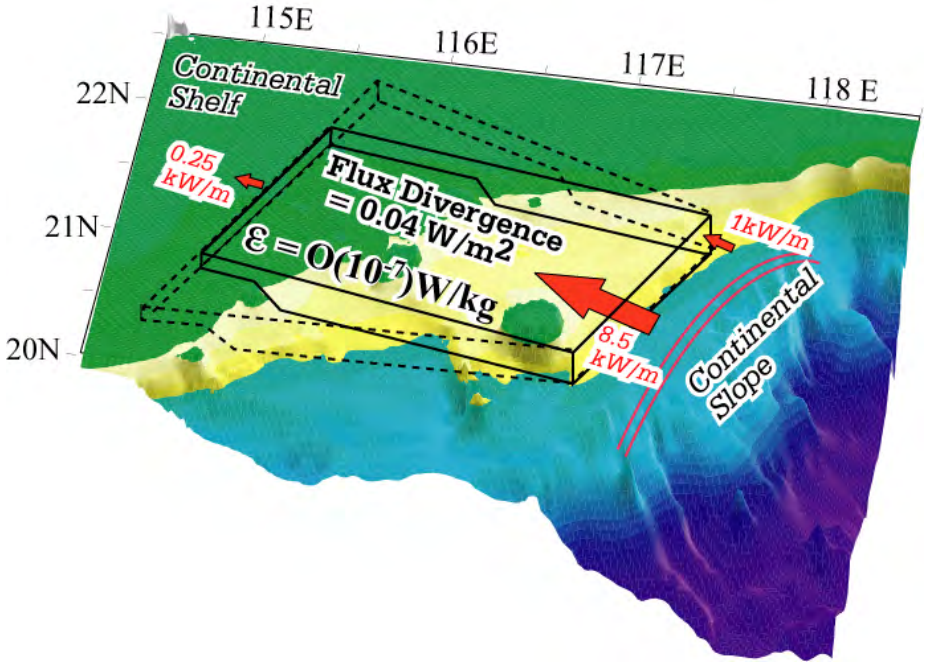

Figure 4: Flux divergence of NLIWs on Dongsha Plateau. The average dissipation rate is calculated as $\varepsilon = \frac{\Delta F}{\Delta s}$***, where*** ΔF ***is the difference between the vertically integrated energy flux of NLIWs on the eastern edge of Dongsha Plateau, 8.5 kW*** m^{-1}***, and that on the continental shelf, 0.25 kW*** m^{-1}***, and*** Δs ***is the distance between the two stations. The flux divergence is ~0.04 W*** m^{-2}***, corresponding to a dissipation rate of O(*** 10^{-7}***) W*** kg^{-1} ***for NLIWs. The dashed-line and solid-line boxes illustrate the horizontal spreading of NLIWs energy.***

Trapped Core Formation within a Shoaling Nonlinear Internal Wave (Lien et al., 2011)

Large-amplitude (100–200 m) non-linear internal waves (NLIWs) were observed on the continental slope in the northern South China Sea nearly diurnally during the spring tide. The evolution of one NLIW as it propagated up the continental slope is captured. The NLIW arrived at the slope as a nearly steady-state solitary depression wave. As it propagated up the slope, the wave propagation speed C decreased dramatically from 2 m s^{-1} to 1.3 m s^{-1}, while the maximum along-wave current speed U_{max} remained constant at 2 m s^{-1}. As U_{max} exceeded C, the NLIW reached its breaking limit and formed a subsurface trapped core with closed streamlines in the coordinate frame of the propagating wave (Fig. 5). The trapped core consisted of two counter-rotating vortices feeding a jet within the core. It was highly turbulent with 10–50-m density overturnings caused by the vortices acting on the background stratification, with an estimated turbulent kinetic energy dissipation rate of $O(10^{-4})$ W kg^{-1} and an eddy diffusivity of $O(10^{-1})$ m^2 s^{-1}. The core mixed continuously with the surrounding water resulting in a wake of mixed water, observed as a salinity anomaly on isopycnals (Fig. 6). As the trapped core

formed, the NLIW became unsteady and dissipative, and broke into a large primary wave and a smaller wave. These processes of wave fission and dissipation continued so that the NLIW evolved from a single deep-water solitary wave as it approached the continental slope into a train of smaller waves on Dongsha Plateau.

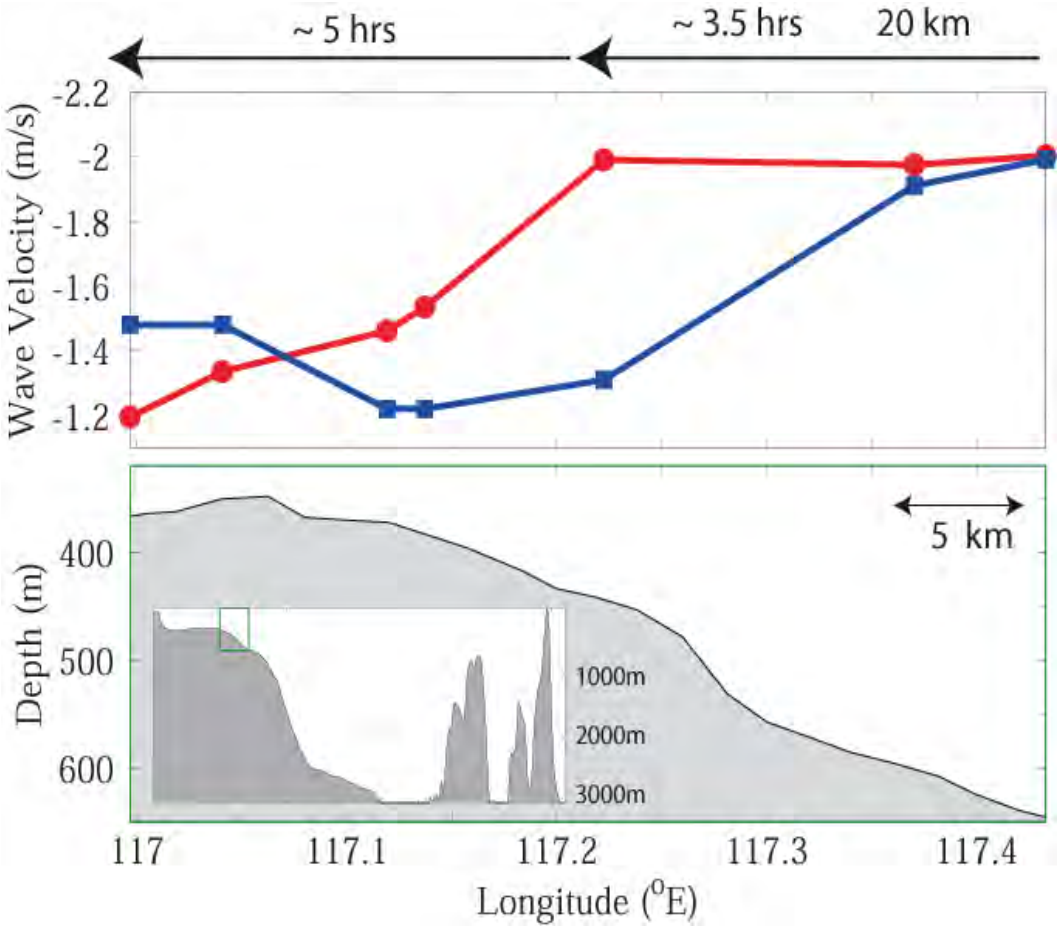

Figure 5: Evolution of maximum current velocity and propagation speed of a NLIW on shoaling topography. The upper panel shows the maximum westward zonal velocity (red curve) and the propagating speed of NLIW (blue curve). The bottom panel shows the bathymetry. The inset is the bathymetry along 21°N in the SCS. A spatial scale of 5 km is shown.

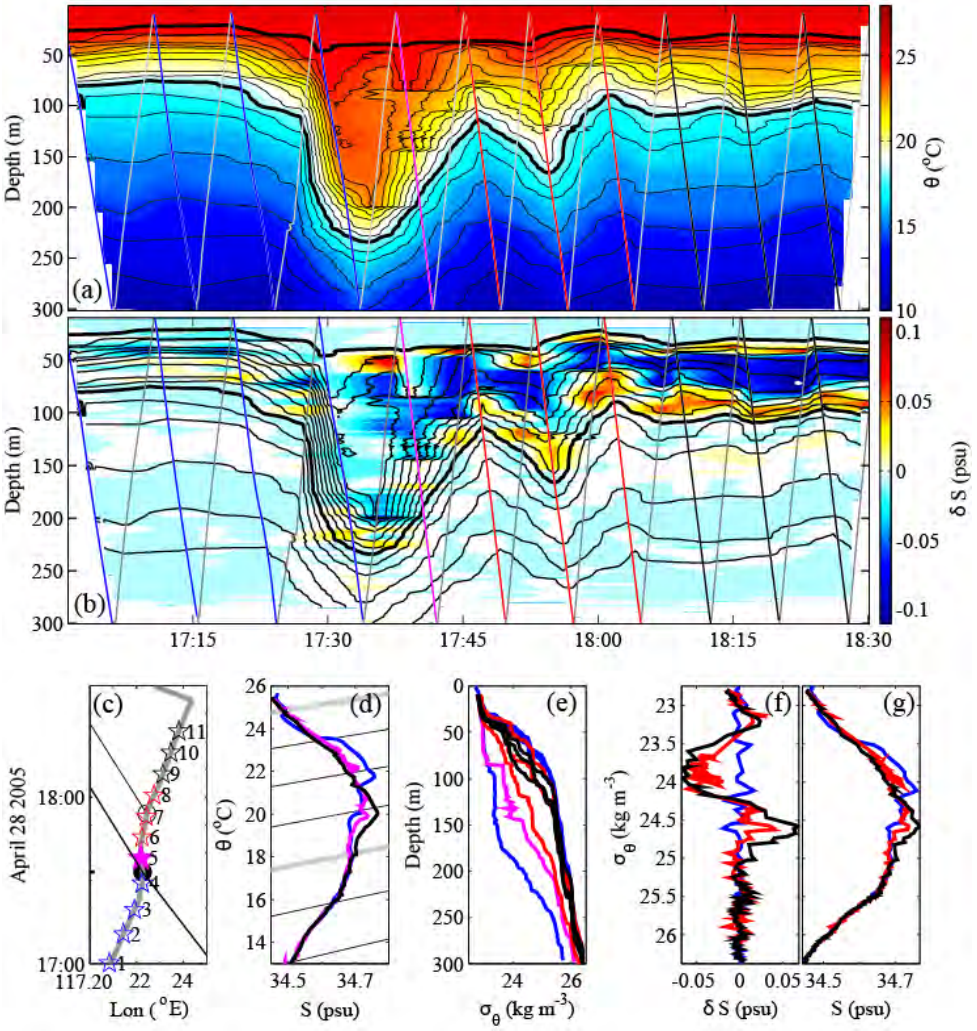

Figure 6: Water mass properties of a trapped core NLIW. (a) Depth-time variation of potential density (contours, interval = 0.2 kg m^{-3}) and potential temperature (colors). (b) Same but for salinity anomaly relative to the first CTD downcast. The zigzag vertical profiles show the trajectory of the shipboard CTD. The two thick black density contours, σ_θ = 23 and 25 kg m^{-3}, identify the range influenced by the trapped core. (c) Time and positions of yoyo CTD downcasts (stars) labeled by number of casts and color coded. The thick and open dots represent the leading NLIW and a small secondary wave. The black line represents the NLIW path. (d) Potential temperature–salinity plot for selected profiles before (blue), during (red), and after (black) NLIW passage. Thin black lines are isopycnals. Thicker grey lines are trapped core boundaries. (e) Same but for potential density profiles. (f) Same but for salinity anomaly against potential density. (g) Same but for salinity against potential density. Blue, red, and black curves in (d), (f), and (g) represent 1st, 5th, and 11th CTD downcasts, respectively. The colors of curves in (e) correspond to those of CTD tracks shown in (b).

<u>Nonlinear Internal Wave Properties Estimated with Shipboard Radar Measurements (Chang et al. 2008)</u>

Surface waves are modulated by NLIWs. In the SCS the interaction is extremely strong due to the

large horizontal velocity convergence of NLIWs (Chang et al. 2008). The shipboard marine radar reveals the strongest scattering strength corresponding to the strongest horizontal velocity convergence measured by the shipboard ADCP.

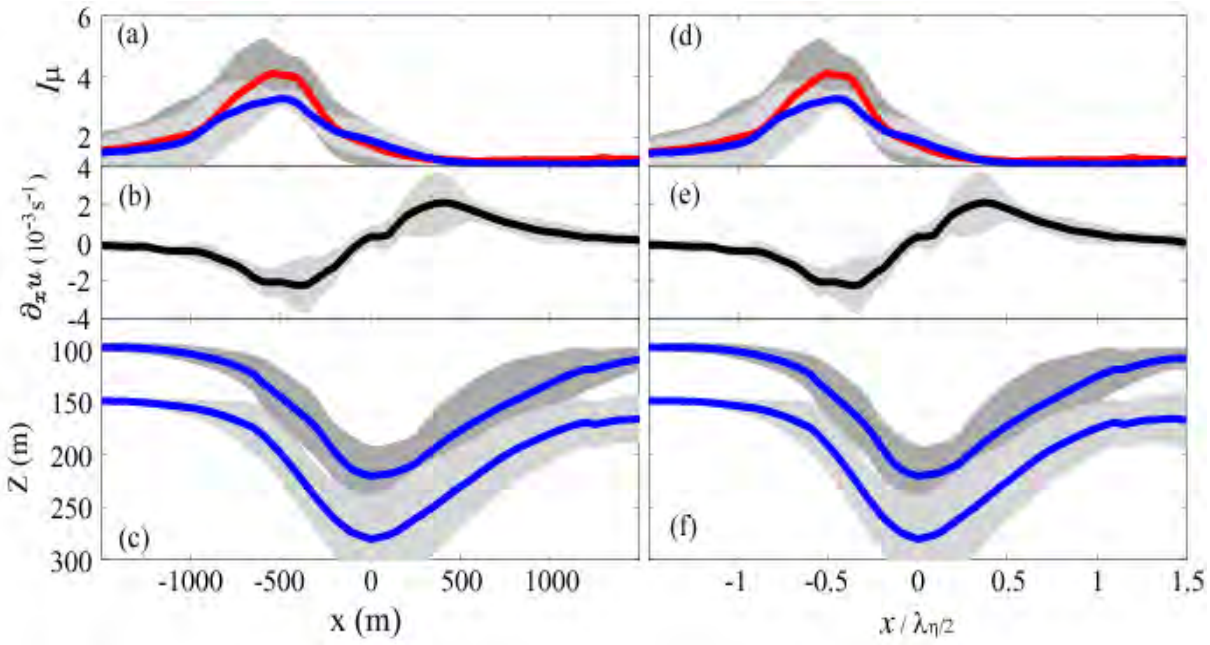

Figure 7: (a) Surface scattering strength, (b) horizontal velocity convergence, and (c) vertical displacement of NLIWs at initial depths of 100 and 150 m averaged over seven NLIW events. (d)–(f) are the same as (a)–(c) except that the x-axis is scaled by the wave width of the half maximum amplitude. Red curves in (a) and (d) represent the surface scattering strength observed from ahead of the propagating NLIWs and the blue curves represent the surface scattering strength observed from behind the propagating NLIWs. The light gray and heavy gray shadings represent 95% confidence intervals.

A composite view of the sea surface scattering strength, the horizontal velocity convergence, and the vertical displacement of NLIWs (Fig. 7) shows the strongest surface scattering strength at the front portion of the NLIW, ~0.5 $\lambda_{\eta/2}$, where $\lambda_{\eta/2}$ is the wave-width at half of the maximum amplitude.

An empirical formula between the surface scattering strength and horizontal velocity convergence (Fig. 8) shows a linear relation at low horizontal velocity convergence that reaches an asymptotic value at high horizontal velocity convergence, indicating a saturation state presumably due to breaking surface waves. Following the power-law and the linear fits between the scattering strength and the local wind speed, the maximum surface scattering enhancement by NLIWs is equivalent to that caused by a wind of ~6 m s^{-1} with surface waves of ~1.5 m, according to the Beaufort wind scale. In other words, the surface scattering enhancement induced by NLIWs will be overwhelmed by that induced by the wind and cannot be identified with the X-band radar when the wind is stronger than 6 m s^{-1}. The vertical displacement of NLIWs is found to be proportional to the spatial integration of the surface scattering strength. In the low-wind condition remote sensing measurements may provide useful predictions of horizontal velocity convergences, amplitudes, and spatial structures of NLIWs.

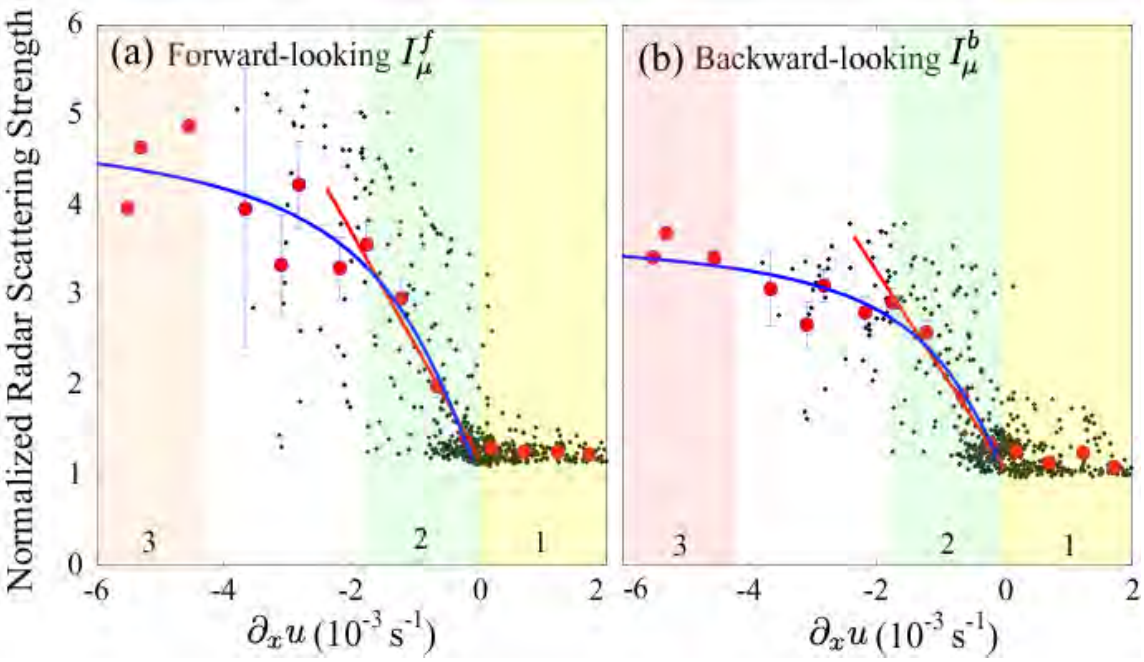

Figure 8: Scatter plots and model fits between the surface scattering strength and the horizontal velocity convergence computed from shipboard ADCP measurements. (a) Observations (gray dots) taken ahead of the propagating NLIWs. Red dots represent averages over constant intervals of horizontal convergence 0.005 s^{-1}. Vertical lines represent 95% confidence intervals. Red and blue curves represent the linear and arctangent fits to observations (red dots). Three regions labeled as 1, 2, and 3 represent the divergence zone, the weak convergence zone, and the strong convergence zone, respectively. Symbols, curves, and labels in (b) are the same as in (a), but observations were taken behind the propagating NLIWs.

Nonlinear Internal Wave Properties Estimated with Moored ADCP Measurements (Chang et al. 2011)

A method is developed to estimate NLIW vertical displacement, propagation direction, and propagation speed from moored ADCP velocity observations. The method is applied to three sets of bottom-moored ADCP measurements taken on the continental slope in the South China Sea in 2006–2007. NLIW vertical displacement is computed as the time integration of ADCP vertical velocity observations corrected with the vertical advection of the background flow by the NLIW. NLIW vertical currents displace the background horizontal current and shear by ~150 m. NLIW propagation direction is estimated as the principal direction of the wave-induced horizontal velocity vector. And propagation speed is estimated using the continuity equation in the direction of wave propagation, assuming the wave horizontal spatial structure and propagation speed remain constant as the NLIW passes the mooring, typically *O*(10 min). These NLIW properties are estimated simultaneously and iteratively using the ADCP velocity measurements corrected for their beam-spreading effect. For most cases, estimates converge to within 3% after four iterations. This method of extracting NLIW properties from velocity measurements is further confirmed using NLIWs simulated by the fully nonlinear Dubreil–Jacotin–Long model. Estimates of propagation speed using the ADCP velocity measurements are also in good agreement with those calculated from NLIW arrival times at successive moorings. This study concludes that velocity measurements taken from a single moored ADCP can provide useful estimates of vertical displacement, propagation direction, and propagation speed of large-amplitude NLIWs.

IMPACT/APPLICATION

Our analysis concludes that NLIWs evolve rapidly across the upper flank of the continental slope and Dongsha Plateau via complicated processes, e.g., the formation of trapped cores and the development of wave trains. These processes are responsible for the strong dissipation of NLIWs in the SCS. Our analysis of combined remote sensing and in-situ measurements yields a model to predict NLIW properties applicable to satellite observations. The newly developed scheme to estimate NLIW wave speed and direction is useful for quantifying the wave properties, including energy flux, using a single bottom-mounted ADCP. The analysis of long-term observations of NLIWs in the vicinity of Dongsha Plateau is in progress and will provide a better prediction of NLIWs in the SCS.

TRANSITIONS

None

RELATED PROJECTS

Study of Kuroshio Intrusion and Transport Using Moorings, HPIES, and EM-APEX Floats (N00014-08-1-0558) as a part of QPE DRI: The primary objectives of this observational program are 1) to quantify and to understand the dynamics of the Kuroshio intrusion and its migration into the southern East China Sea (SECS), 2) to identify the generation mechanisms of the Cold Dome often found on the SECS, 3) to quantify the internal tidal energy flux and budgets on the SECS and study the effects of the Kuroshio front on the internal tidal energy flux, 4) to quantify NLIWs and provide statistical properties of NLIWs in the SECS , and 5) to provide our results to acoustic investigators to assess the uncertainty in acoustic predictions.

Process Study of Oceanic Responses to Typhoons using Arrays of EM-APEX Floats and Moorings (N00014-08-1-0560) as a part of ITOP DRI: We study the dynamics of the oceanic response to and recovery from tropical cyclones in the western Pacific using long-term mooring observations and an array of EM-APEX floats. Pacific typhoons may cause cold pools on the continental shelf of the East China Sea.

REFERENCES

Zhao, Z., V. Klemas, Q. Zheng, and X.-H. Yang, Remote sensing evidence for baroclinic tide origin of internal solitary waves in the northeastern South China Sea, *Geophys. Res. Lett.*, **31**, L06302, doi:10,1029/2003GL019077, 2004.

PUBLICATIONS

Lien, R.-C., T. Y. Tang, M. H. Chang, and E. A. D'Asaro, Energy of nonlinear internal waves in the South China Sea, *Geophys. Res. Lett.*, **32**, L05615, doi:10.1029/2004GL022012, 2005.

Chang, M.-H., R.-C. Lien, T. Y. Tang, E. A. D'Asaro, and Y. J. Yang, Energy flux of nonlinear internal waves in northern South China Sea, *Geophys. Res. Lett.*, **33**, L03607, doi:10.1029/2005GL025196, 2006.

Moore, S. E., and R.-C. Lien, Pilot whales follow internal solitary waves in the South China Sea, *Mar. Mamm. Sci.*, **23**, 1, 193–196, 2007.

Chang, M.-H., R.-C. Lien, T. Y. Tang, Y. J. Yang, and J. Wang, A composite view of surface signatures and interior properties of nonlinear internal waves: Observations and applications, *J. Atmos. Ocean. Technol.*, **25**, 1218-1227, 2008.

Chang, M.-H., R.-C. Lien, Y. J. Yang, and T. Y. Tang, Nonlinear internal wave properties estimated with moored ADCP measurements, *J. Atmos. Ocean. Technol*., in press, 2011.

Lien, R.-C., E. A. D'Asaro, F. Henyey, M.-H. Chang, T. Y. Tang, and Y. J. Yang, Trapped core formation within a shoaling nonlinear internal wave, submitted to *J. Phys. Oceanogr*., 2011.